

Article

The Antennal Sensory Structures of Female *Anagyrus vladimiri* (Hymenoptera: Encyrtidae)

Milos Sevarika ¹, Paolo Giannotti ², Andrea Lucchi ² and Roberto Romani ^{1,*}¹ Department of Agricultural, Food and Environmental Sciences, University of Perugia, 06121 Perugia, Italy² Department of Agriculture, Food and Environment, University of Pisa, 56124 Pisa, Italy

* Correspondence: roberto.romani@unipg.it; Tel.: +39-075-585-6032

Simple Summary: Perception of olfactory cues represents a core function of insects. They perceive these signals by small organs, termed as sensilla, mostly located on the antennae. Besides olfactory sensilla, the antennae are also equipped with other types of sensilla involved in the perception of various cues (i.e., contact chemical, mechanical, physical). Through the integration of different stimuli from the environment, insects are able to interact dynamically with the biotic and abiotic components of the ecosystem. The ultrastructural characterization of sensilla allows for a specific function to be assigned to a specific type of sensilla, providing the base for further electrophysiological and ecological studies. In this work, we investigated the antennae of an important biocontrol agent of scale insects, *Anagyrus vladimiri*. The ultrastructural organization of the sensilla was investigated by scanning and transmission electron microscopy. We found eight different types of antennal sensilla, for which we proposed a specific functional hypothesis.

Abstract: The Encyrtidae (Hymenoptera) encompasses a large group of parasitic wasps widely used in biocontrol programs of scale insects (Hemiptera: Coccoidea). *Anagyrus vladimiri* is a solitary parasitoid that attacks and develops on several mealybugs of economic importance. Thus, this species is widely used as a biocontrol agent of *Planococcus* spp. and *Pseudococcus* spp. *A. vladimiri* males and females show sexual dimorphism with regard to the antennal organization, in terms of shape and the development of antennomeres. Ultrastructural investigations of female antennae, carried out with scanning (SEM) and transmission (TEM) electron microscopy, revealed the presence of nine distinct antennomeres. The scape was enlarged and paddle-like, compared to the other antennomeres. The club (the apical antennomere) was mono-segmented and housed the highest number of sensilla. Eight morphologically different types of sensilla were described; sensilla trichoidea I, trichoidea II, chaetica I, chaetica II, grooved peg sensilla, campaniform sensilla, multiporous plate sensilla and multiporous basiconic sensilla. Ultrastructural investigations allowed for us to assign a specific function to each type of sensilla. The most abundant type of sensilla were sensilla trichoidea I and multiporous plate sensilla. We also found two types of sensilla (multiporous basiconic sensilla and sensilla chaetica II) that were present only on the females.

Keywords: SEM; TEM; ultrastructure; parasitoid; sensilla

Citation: Sevarika, M.; Giannotti, P.; Lucchi, A.; Romani, R. The Antennal Sensory Structures of Female *Anagyrus vladimiri* (Hymenoptera: Encyrtidae). *Insects* **2022**, *13*, 1138. <https://doi.org/10.3390/insects13121138>

Academic Editor: Sylvia Anton

Received: 12 November 2022

Accepted: 8 December 2022

Published: 10 December 2022

Publisher's Note: MDPI stays neutral with regard to jurisdictional claims in published maps and institutional affiliations.



Copyright: © 2022 by the authors. Licensee MDPI, Basel, Switzerland. This article is an open access article distributed under the terms and conditions of the Creative Commons Attribution (CC BY) license (<https://creativecommons.org/licenses/by/4.0/>).

1. Introduction

The mealybugs (Hemiptera: Pseudococcidae) are a group of scale insects, recognized as important pests of agricultural and ornamental crops [1]. They cause damage as nymphs and adults by inhibiting plant growth, excreting large quantities of honeydew, causing defoliation, plant damage and ultimately loss in production [2,3]. In addition, they are known as vectors of plant viruses [4,5]. The detection and control of mealybugs are challenging, due to their cryptic behaviour and wax production, which serves as a protective barrier against successful insecticide application [6–9]. In the framework of integrated pest management (IPM), different biocontrol agents, including predators (e.g., Coccinellidae) and parasitoids

(Encyrtidae), are used to suppress the mealybug population. Specifically, endoparasitoids from the genus *Anagyrus* are often included in biocontrol programs [8,10–12].

The genus *Anagyrus* encompasses about 350 species of primary endoparasitoid of Pseudococcidae [13]. Within the genus, there are morphologically similar species, such as *Anagyrus pseudococci* (Girault), *A. sp. near pseudococci* (Girault), *A. dactylopii* (Howard), *A. kamali* Moursi and *A. kivuensis* Compere. All these species are nominally included in the informally designated *Anagyrus pseudococci* complex, distinguished by the coloration of the female antennal flagellomere 1 (F1) [14]. Because of their morphological similarity, the first two species have been misidentified and are sometimes confused or mistaken for each other by researchers and commercial bio-factories.

Previous research discovered a variation in F1 coloration on female parasitoids between Californian (completely black morphotype) and Argentinian (black/white morphotype) populations. Primarily, it was believed that this minor variation could represent population-specific characteristics. However, further analysis confirmed that the taxon formerly defined as *A. pseudococci* conversely included a different species that was initially classified as *A. sp. near pseudococci* (Girault) [15] and then described and named as *Anagyrus vladimiri* Triapitsyn [14].

A. vladimiri is a well-known biocontrol agent of *Planococcus* spp. and *Pseudococcus* spp. species. Until now, it has been successfully used to control *Pseudococcus comstocki* (Kuwana), *P. viburni*, *Planococcus ficus* (Signoret) and *P. citri* [15,16].

The success of a biocontrol agent in controlling a pest is partially correlated with its ability to locate a host in an appropriate time window. To do so, insects utilize diverse cues, of which olfactory plays a major role. Some olfactory cues are highly volatile and thus detected through larger distances (pheromones, oviposition induced plant volatiles (OIPV), herbivore induced plant volatiles (HIPV)), contrasting with the less or even non-volatile, like in the case of cuticular hydrocarbons. Volatile cues are detected by olfactory sensilla, while non-volatile by gustatory sensilla [17–19]. These, along with other sensilla (mechanoreceptors, thermo-hygroreceptors), are present all over the insect body, but mainly on the antennae, which are recognized as the primary sensory appendages [20].

The morphology and distribution of antennal sensilla in males and females of *A. vladimiri* have been studied with the scanning electron microscopy [21]. Six morphologically different sensilla were found on both sexes: trichoidea, placoidea, basiconica and chaetica type 1, type 3 and type 4, whereas chaetica type 2 sensilla were present only in females, and tridentate scale-shaped-type sensilla were present only in males. Based on sensilla external morphology (the presence or absence of pores), authors have hypothesized a possible olfactory, gustatory or mechanoreceptive function.

In our work, we studied in detail the antennae of *A. vladimiri* with both scanning and transmission electron microscopy, with the aim to define the possible real function of sensilla in the female antennae.

2. Materials and Methods

2.1. Insects

Commercially mass-reared males and females of *A. vladimiri* were provided by Bio-Planet (Cesena, Italy). When emerged, parasitoids were sexed, independently stored in clean glass vials and fed with a tiny drop of water and honey solution (1:1).

2.2. Scanning Electron Microscopy (SEM)

Ten *A. vladimiri* adult females and males were used. The insects were anesthetized by freezing and their head capsules, complete with the antennae, were excised from the thorax using fine forceps and placed in a lens cleaner liquid for 24 h. Dehydration was carried out in a graded series of ethanol (from 50% up to 99%) followed by treatment with a critical point dryer Leica EM CPD 030 (Leica Microsystems, Wetzlar, Germany). Then, the specimens were mounted on aluminium stubs with double-sided sticky tape, positioned on dorsal or ventral sides to obtain a total sensillar count for each replicate. The specimens

were then sputter-coated with an Edwards sputter coater S150B (BOC Edwards, Burgess Hill, UK) prior to their examination with a Scanning Electron Microscope FEI Quanta 200 (Thermo Fisher Scientific Inc., Hillsboro, OR, USA).

2.3. Transmission Electron Microscopy (TEM)

For TEM observations, five females were paralyzed by exposure to cold temperatures ($-18\text{ }^{\circ}\text{C}$) for 60 s, then immediately immersed into a solution of glutaraldehyde and paraformaldehyde 2.5% in 0.1 M cacodylate buffer +5% sucrose, pH 7.2–7.3. Each antenna was detached from its base, single antennomeres were isolated and reduced in size by cutting them in two parts to facilitate fixative penetration and then left at $4\text{ }^{\circ}\text{C}$ for 2 h. The specimens were kept at $4\text{ }^{\circ}\text{C}$ overnight in the same buffer, then they were post-fixed in 1% OsO₄ (osmium tetroxide) for 1 h at $4\text{ }^{\circ}\text{C}$ and rinsed in the same buffer. Dehydration, in a graded ethanol series from 60% to 99%, was followed by embedding in Epon-Araldite (Sigma-Aldrich, Dorset, UK) with propylene oxide as a bridging solvent. Thin sections were taken with a diamond knife on a LKB “Nova” ultramicrotome (LKB, Stockholm, Sweden) and mounted on 50 formvar-coated mesh grids. Then, sections on the grids were stained with uranyl acetate (20 min, room temperature) and lead citrate (5 min, room temperature). Finally, the sections were observed with a Philips[®] EM 208 (Thermo Fisher Scientific Inc., Hillsboro, OR, USA). Digital pictures (1376×1032 pixels, 8 bit, uncompressed greyscale TIFF files) were obtained using a high-resolution digital camera MegaViewIII (SIS[®]) (SIS, Muenster, Germany) connected to the TEM.

3. Results

3.1. General Description of the Antennae

The antennae of female *A. vladimiri* were the typical antennae found in Hymenoptera, characterised by a geniculate structure and inserted frontally on the head capsule, below the compound eyes and close to the mouthparts. Each antenna was made up of a scape, a pedicel and a flagellum composed of seven flagellomeres (F1–F7); therefore, the whole antenna was made of nine antennomeres (Figure 1A). The scape was inserted in the head capsule through an elliptical socket (Figure 2A). The basal part of the scape was cylindrical and relatively short. At this level, sensilla trichoidea were found arranged close to the head–scape joint (Figure 2A). The most evident region of the scape started in the form of a paddle-like structure, laterally flattened and covered by numerous long hairs (Figure 1A). No pores were found on both sides of any region of the scape. The cuticular surface of the scape presented an elaborate, scale-like sculpture. Occasionally, a few curls of wax originating from the attacked host were observed. The pedicel was attached to the apical corner of the scape, opposite to the rounded edge. Sensilla trichoidea, similar in shape and arrangement to those reported at the head–scape joint, were visible at the scape–pedicel joint (Figure 2B). The pedicel appeared conical in shape, with the diameter increasing from the proximal to the distal part, where sparse campaniform sensilla were found (Figure 2C). Antennomeres ranging from F1 to F6 were cylindrical in shape and similar in size (Figure 1A). The last antennomere (F7) was club-like and resulted from the merging of three originally separated antennomeres (Figure 1A–C). It was the largest antennomere of the antenna—about $180\text{ }\mu\text{m}$ long.

In males, the antenna is made of the same number of antennomeres, but has a different general structure, being longer and slender compared to the female one (Figure 1D). The scape was much smaller and did not show the paddle-like shape. The apical part of the antenna was not clubbed and a single row of scale-like structures was presented on its ventral side (Figure 1E).

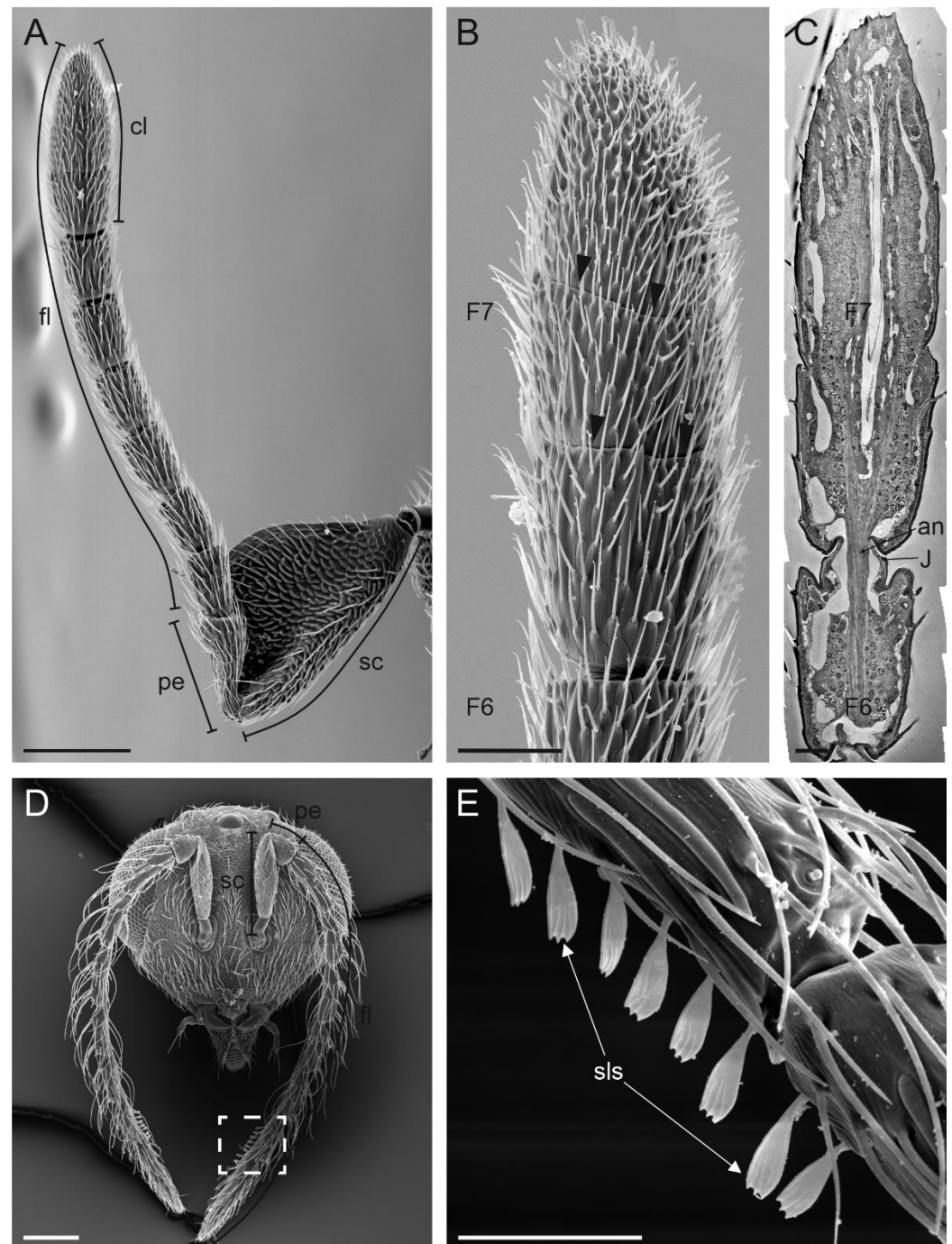


Figure 1. Scanning electron microscopy (SEM) of the *Anagyrus vladimiri* antennae. **(A)** General view of the female antenna showing the paddle-like scape (sc), the pedicel (pe) and the flagellomere made up of seven antennomeres. **(B)** Detail of the 7th flagellomere (F7), forming the apical club (cl). Two transverse furrows are indicated by black arrowheads. **(C)** Transmission electron microscopy image obtained combining 13 adjacent pictures, showing a longitudinal section of the F7 and F6. The dissection plan is positioned at the level of the medial region of the antenna, clearly showing the absence of segments at the F7 outer-grooves level. **(D)** SEM picture showing the male head capsule with the two antennae made of 9 antennomeres. **(E)** Close-up view of the dotted square in **(D)** depicting a detail of the scale-like structures (SLS) occurring ventrally on the last two antennomeres. An: antennal nerve; j: joint. Scale bar: **(A,D)**: 100 μm ; **(B)**: 25 μm ; **(C)**: 10 μm ; **(E)**: 30 μm .

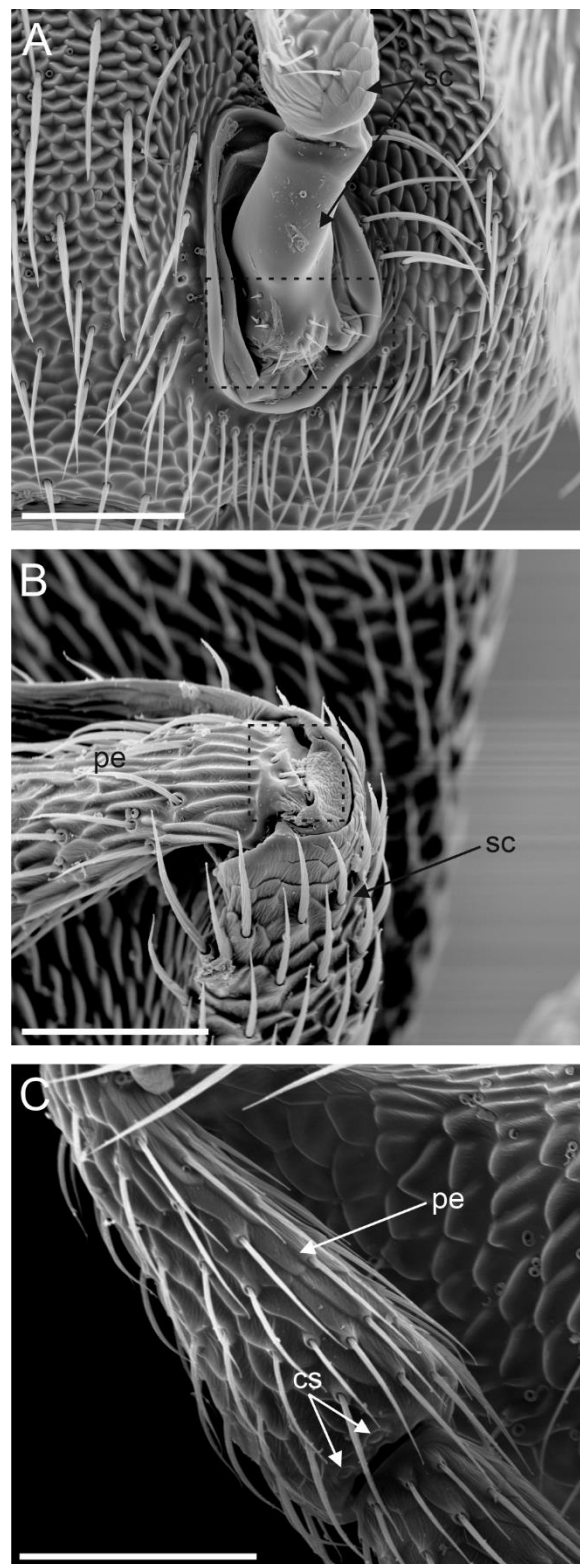


Figure 2. Scanning electron microscopy (SEM) of the *Anagyryus vladimiri* female antennae. (A) There is particular focus on the antenna articulation base at the head capsule. The base of the scape is connected with the torulus. The dotted square shows the area where mechanosensory hairs are positioned. (B) Detail of the scape (sc)–pedicel (pe) joint; at this level, a few mechanosensory hairs are located near the articulation joint (dotted square). (C) Lateral view of the pedicel (pe): two campaniform sensilla (CS) are positioned at the distal end of the antennomere. Scale bar: (A,C): 50 μm ; (B): 40 μm .

3.2. Type of Sensilla

Morphological analysis revealed the presence of eight types of sensilla, which were classified according to their ultrastructural features. A scheme reporting the different sensilla and their distribution along the antennomeres is reported in Figure 3.

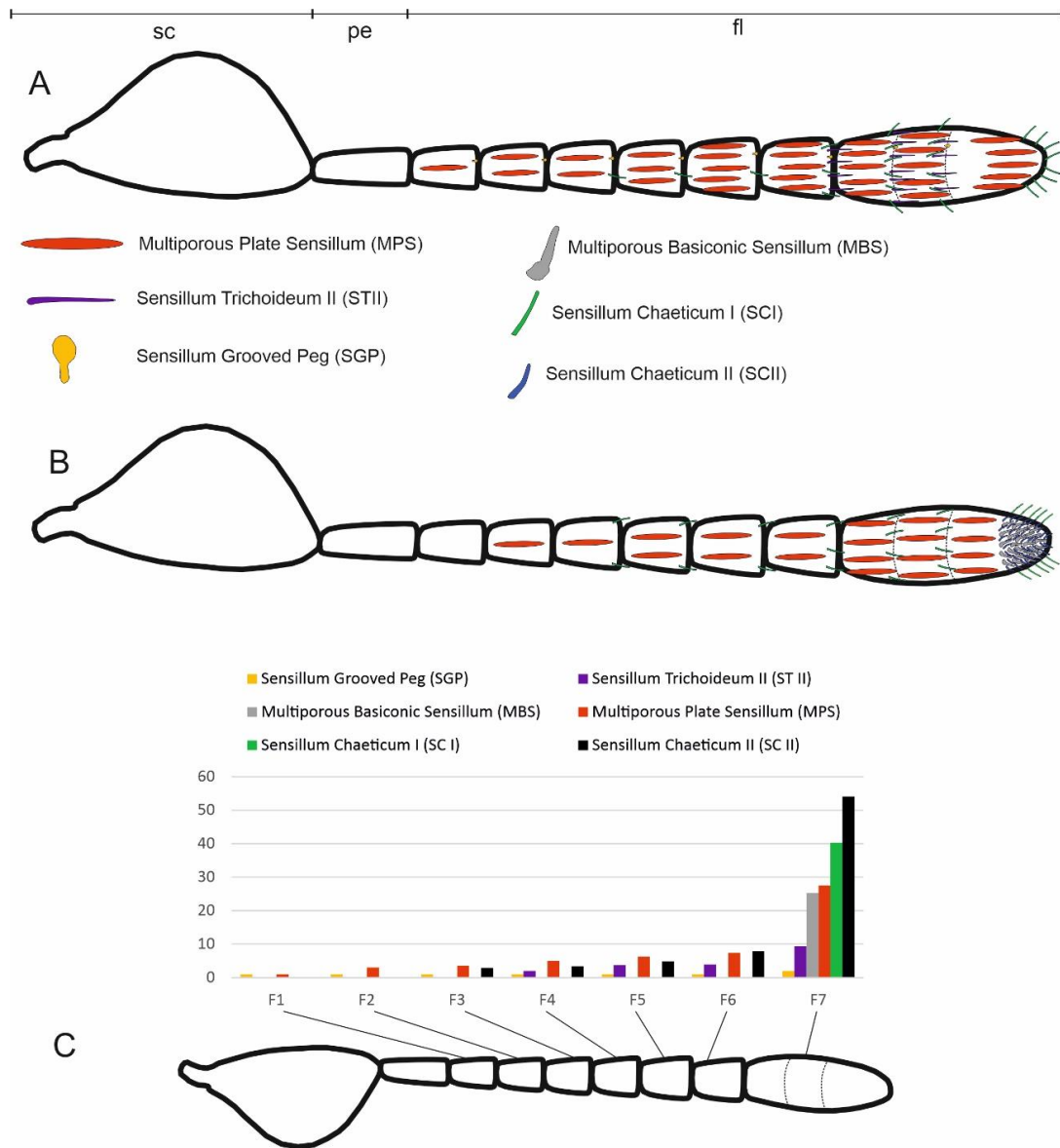


Figure 3. Schematic drawing of *Anagyrus vladimiri* female antennae from dorsal (A) and ventral (B) views. The different types of sensilla are reported with their relative distribution. Sensilla trichoidea I are omitted. (C) Graph showing the relative abundance of the different sensilla types on the different flagellomeres (numbered from F1 to F7). Sc, scape; pe, pedicel; fl, flagellum.

3.3. Sensilla Trichoidea I (ST I)

Sensilla trichoidea I were the most abundant sensilla on the female antennae. They were present on all antennomeres and arranged in a sequence on both dorsal and ventral sides (Figure 4A). ST I were about 15 µm long and had a bristle-like shape. The external cuticular wall was crossed by longitudinal, shallow furrows throughout its length. The presence of pores was not recorded in ST I (Figure 4B). This characteristic allowed for easy identification from the other subtypes of sensilla trichoidea. At the sensillum base, a distinct socket was present. At this level, TEM cross-sections revealed the presence of a single sensory neuron ending in a tubular body (Figure 4C).

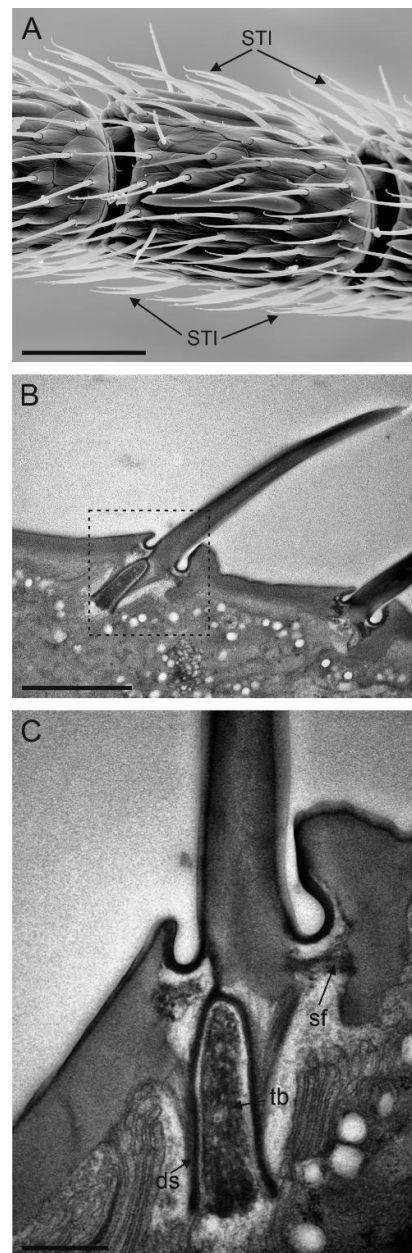


Figure 4. (A) SEM picture of flagellomere 5 (F5) of *Anagyryus vladimiri* female antennae showing the distribution of sensilla trichoidea I (ST I). (B) TEM picture taken longitudinally through the cuticular shaft and base socket. (C) Close-up view of the base socket (dotted square in (B)) showing the suspension fibres and the single sensory neuron ending in a tubular body (tb) encased by the dendrite sheath (DS). Scale bar: (A): 30 μm ; (B): 2 μm ; (C): 0.5 μm .

3.4. Sensilla Trichoidea II (ST II)

Sensilla trichoidea II differ from sensilla trichoidea I by being present on the antennae, starting from the sixth antennomere (F4) (Figure 5A). Their number gradually increased from two on F4 to ten on F7. ST II were slightly wider and longer than ST I (about 18 μm in length) and inserted through the antennal wall with an inflexible socket (Figure 5A). Moreover, their external cuticle appeared to be smooth, pierced by tiny pores, mostly organised in parallel lines. The tip was slightly rounded (Figure 5B). A cross-section taken at the apical part of the sensillum revealed the presence of the branched sensory neurons filling the sensillum lumen (Figure 5C). The cuticular wall was thick (~300 nm) and with a few pores (Figure 5C). Sections taken at the basal part of the sensillum showed the presence of five sensory neurons (Figure 5D).

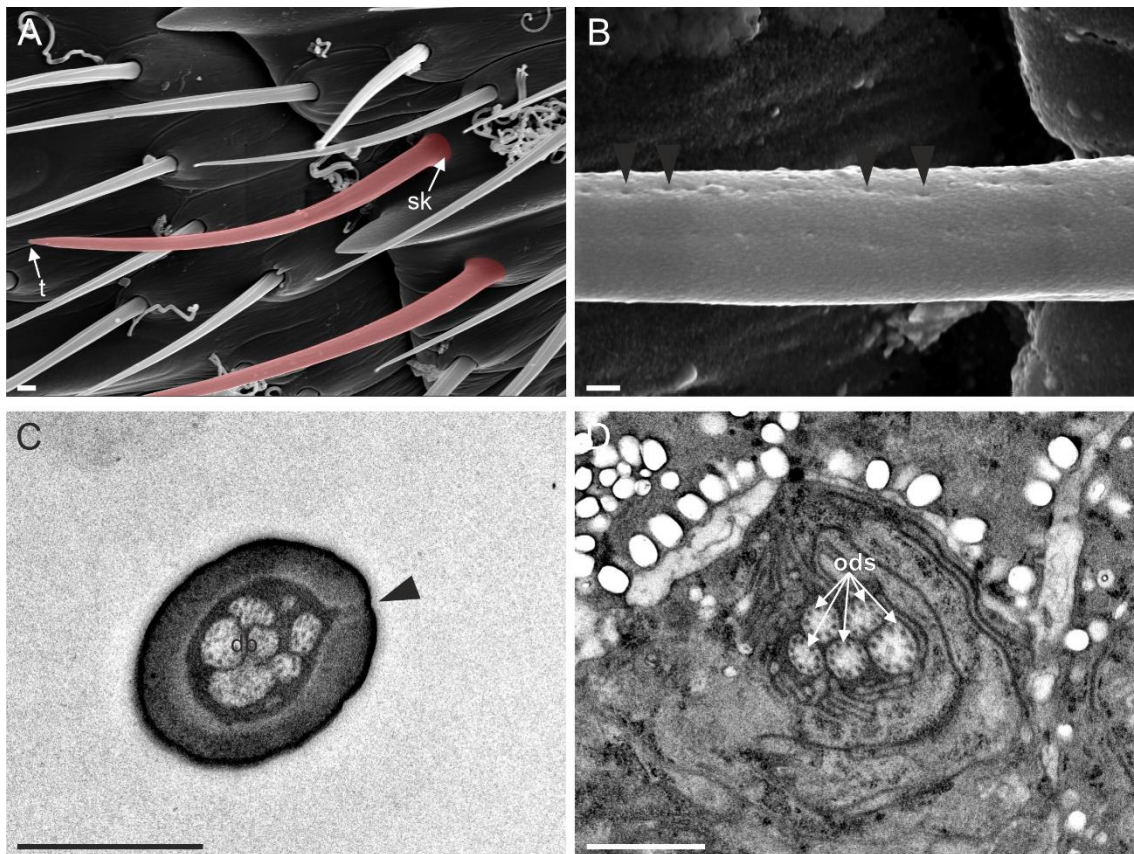


Figure 5. (A) SEM picture of the distal area of flagellomere 5 (F5) female antennae in *Anagyrus vladimiri*, two sensilla trichoidea II (ST II) are visible—highlighted with a red mask. The pointed tip (t) and the inflexible socket (sk) are clearly visible. In (B), a series of cuticular pores on the surface of ST II can be observed (black arrowheads). (C) TEM picture showing a cross-section of an ST II, the section is taken approximately at the medial region of the sensillum. The lumen is occupied by a series of dendritic branches (db), while a pore is visible, connecting the sensillar lumen with the outside (black arrowhead). (D) TEM picture of the same sensillum in (C) taken below the sensillum base; five outer dendritic segments (ods) belonging to the sensory neurons innervating the sensillum are visible. Scale bar: (A,C,D): 1 μm ; (B): 0.2 μm .

3.5. Multiporous Plate Sensilla (MPS)

Multiporous plate sensilla were flattened structures that presented a slightly elevated medial part. MPS were longitudinally positioned over the antennomeres and were evenly distributed over the dorsal and ventral side of the antennae (Figure 6A). These sensilla were absent on the scape and the pedicel but present on all flagellomeres. The number of the sensilla gradually increased, being highest at the apical antennomere, where about 28 sensilla were observed. The sensilla were about 42 μm in length. Generally, the sensilla extended over a single antennomere; however, sometimes the sensillum tip protruded over the next antennomere (Figure 6A,C). A close-up view of the external cuticle revealed a sensory cuticle covered by numerous, evenly distributed pores. The transmission electron images revealed the sensillum ultrastructural organization characterized by the multiporous cuticular wall and numerous dendrites (Figure 6C,D). The cross-section images taken at the apical part of the sensillum showed the presence of numerous dendritic branches, while sections taken at the level of the sensory neurons' inner dendritic segment revealed 20–21 units innervating each MPS (Figure 6E).

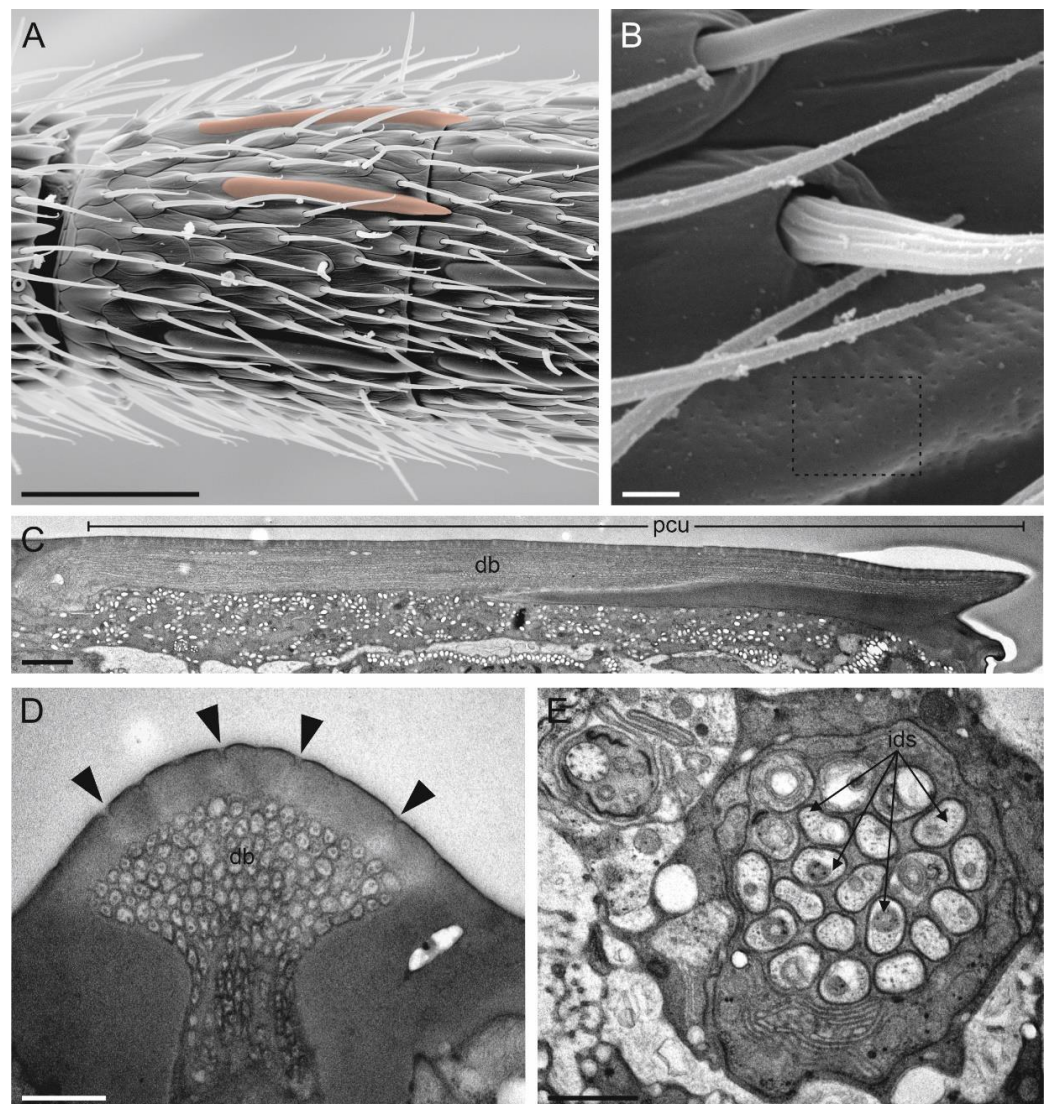


Figure 6. (A) SEM picture of the proximal part of F7 in dorsal view, where two multiporous plate sensilla (MPS) can be observed (red mask). (B) Detail of the porous cuticle (dotted square). (C) TEM image obtained combining 7 adjacent pictures, showing a longitudinal section of an MPS. A large amount of dendrite branches (db) completely fills the space below the porous cuticle (pcu). (D) TEM cross-section of an MPS taken approximately at the third distal length form the tip, showing the cuticular pores (black arrowheads) and the dendrite branches (DB). (E) TEM cross-section showing the bundle of 20 inner dendritic segments (ids) belonging to the sensory neurons innervating a single MPS. Scale bar: (A): 30 μm ; (B,E): 1 μm ; (C): 2 μm ; (D): 0.5 μm .

3.6. Multiporous Basiconic Sensilla (MBS)

These sensilla were found exclusively on the apical part of the last flagellomere, inserted on the ventral side (Figure 7A). On average, 25 sensilla were recorded. MBS were characterized by a distinct socket, in the form of a raised cylinder (diameter 2.5 μm) on which a cuticular peg was inflexibly inserted (Figure 7B). The peg cuticle was longitudinally grooved throughout its entire length, which, on average, was 5.5 μm . MBS had a slightly curved tip, on which the grooves running along the peg ended in elongated, finger-like projections (Figure 7C). While cuticular pores were not observed along the sensillum shaft, cross-sections taken at the level of the apical part revealed the presence of several pores defining an apical porous cuticle (Figure 7D). The dendritic projections (~20) of the outer dendritic segments were present within the sensillum lumen (Figure 7E). At the sensillum

base, the cuticular wall appeared rather smooth and thick. Each MBS was innervated by ~20 sensory neurons, therefore, they reached the porous cuticle unbranched (Figure 7F).

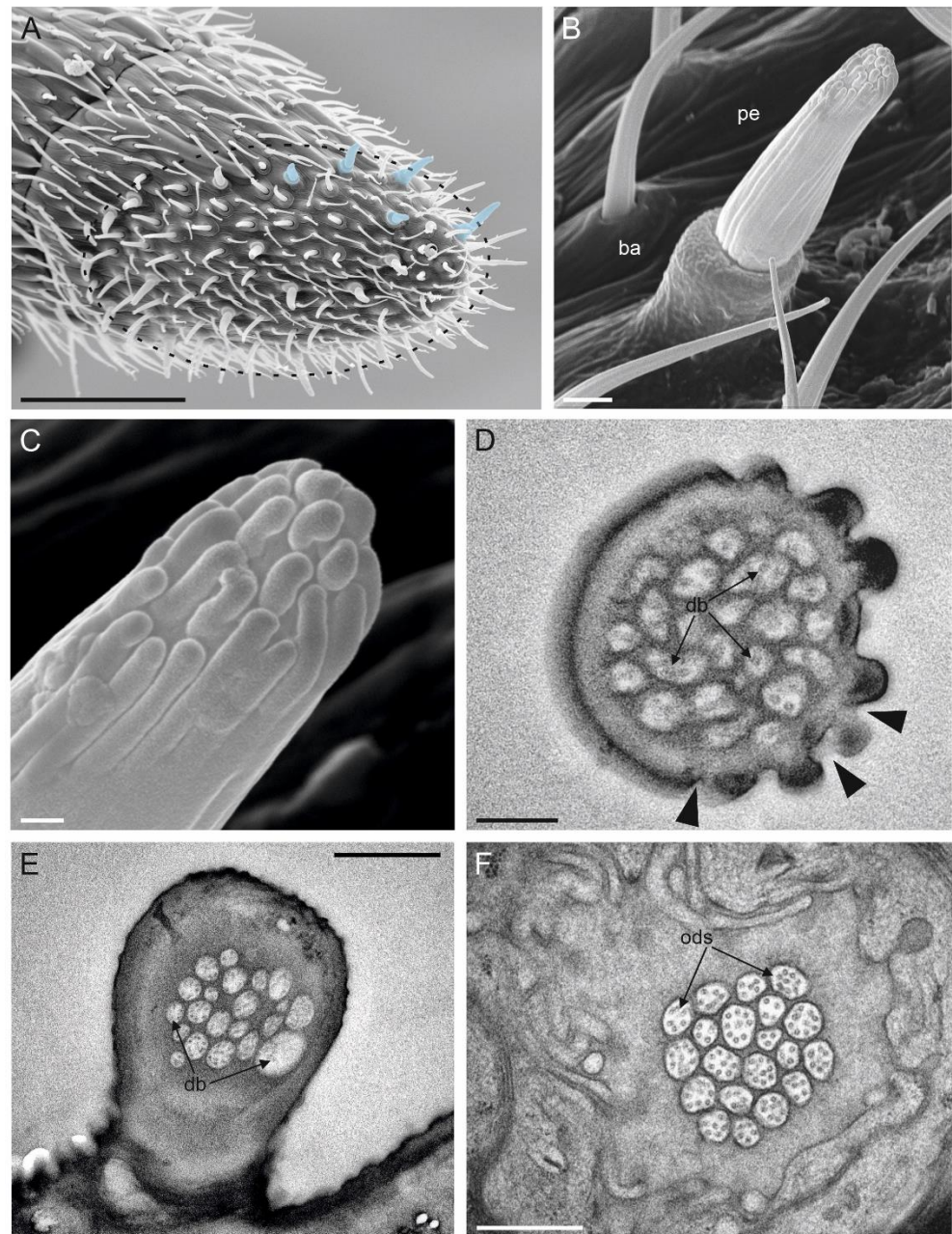


Figure 7. (A) Apical part of the female antenna F7 of *Anagyrus vladimiri* in a ventral view. The apical area appears like a flattened sole where several sensilla are inserted. In the blue mask, some of the multiporous basiconic sensilla (MBS) are highlighted. (B) Detail of MBS at SEM. The sensillum presents a cylindrical base (BA) that is inflexibly inserted on the antennal wall. A grooved peg (pe) is inserted on top of the cylindrical base. (C) Close-up view of the apical region of MBS. The grooves that are present on the cuticular shaft end in elongated finger-like projections. (D) TEM picture showing a cross-section of the apical part of MBS. On the right side, it is possible to observe the finger-like projections and the pores (black arrowheads) partly hidden by the same projections. The internal lumen is filled with dendritic branches (db). (E) TEM section at the basal region of MBS: the cuticular wall appears thicker and aporous, and the same number of db is visible. (F) TEM cross-section through the outer dendritic segments (ODS) of the sensory neurons innervating a single MBS. Scale bar: (A): 30 μm ; (B,E): 1 μm ; (C,D): 0.2 μm ; (F): 0.5 μm .

3.7. Sensilla Chaetica I (SC I)

These sensilla were characterized by their position and shape. They were typically located at the distal part of each antennomere. The SC I were about 15 μm in length and were inserted on the external cuticle with a 45° angle, which distinguished them from other sensilla (Figure 8A). The external wall presented longitudinal grooves over its entire length; no pores were observed. At the sensillum tip, a single pore could be observed (inset in Figure 8A). SC I could be found from F3 to F7, with a pattern displaying an increase in number from the base to the antennal tip (Figure 3). A total of 73 SC I were recorded per antenna, with most of them (54) located on the club (F7). The ultrastructural TEM investigations revealed the presence of a thick, aporous cuticular wall, with evident ridges as a result of the external grooves (Figure 8C). The sensillum housed five sensory neurons enclosed in a dendritic sheath (Figure 8E). Four sensory neurons developed unbranched dendrites that extended into the sensillar lumen (Figure 8C,D). The fifth sensory neuron ended at the tubular body, located at the sensillum base. Moreover, at this level, suspension fibres connected to the flexible socket could be observed (Figure 8B).

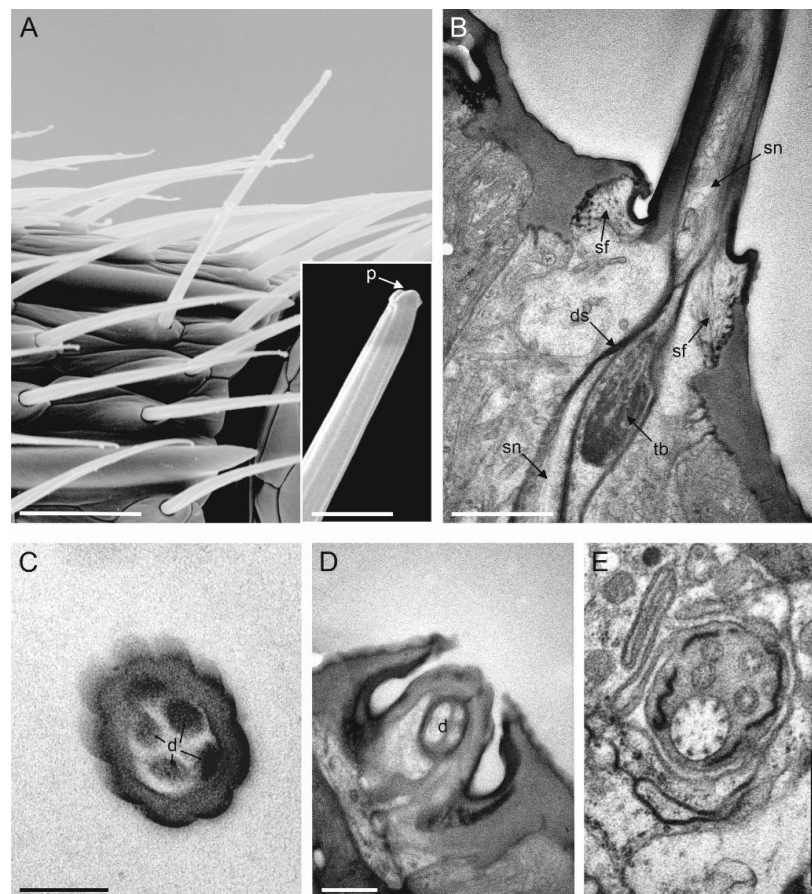


Figure 8. (A) Distal region of F6 *Anagyrus vladimiri* female, with evidence of a single Sensillum Chaeticum I (SC I) protruding from the surrounding STI. SC I is characterized by a grooved shaft and a single apical pore (p) (inset in (A)). (B) TEM cross-section through the socket of a SC I, showing suspension fibres (sf) at the sensillum base and sensory neurons (sn) innervating the sensillum, surrounded by the dendrite sheath (ds). The sensory neurons enter the cuticular shaft of SC I except for the one ending with the tubular body. (C–E) TEM cross-section taken at different levels of an SC I. In (C,D), the sections show the dendrites inside the lumen in the medial region of the cuticular shaft (C) and close to the base (D). In (E), the outer dendritic segments are embedded by a discontinuous dendrite sheath. Note the large dendrite belonging to the mechanosensory unit. Scale bar: A: 10 μm ; inset in (A): 1 μm ; (B,E): 1 μm ; (C): 0.25 μm ; (D): 0.5 μm .

3.8. Sensilla Chaetica II (SC II)

Sensilla chaetica type II were located solely at the apical antennomere; at the same area, MBS were found (Figure 9A). These sensilla showed a cuticular peg characterized by furrows extending over its entire length, ending at the tip and defining an elaborated structure that resembled in part the one reported for MBS (although smaller) (Figure 9B). About 45 sensilla per antenna were recorded, distributed only on the ventral side. The sensilla were inserted on the antennal wall through an evident socket. Although the presence of apical pores was not recorded, we hypothesized the presence of a single pore at the tip. The length on average was 7 μm . Ultrastructural investigations with the TEM revealed the presence of five sensory neurons, of which one ended at the tubular body (Figure 9C,D).

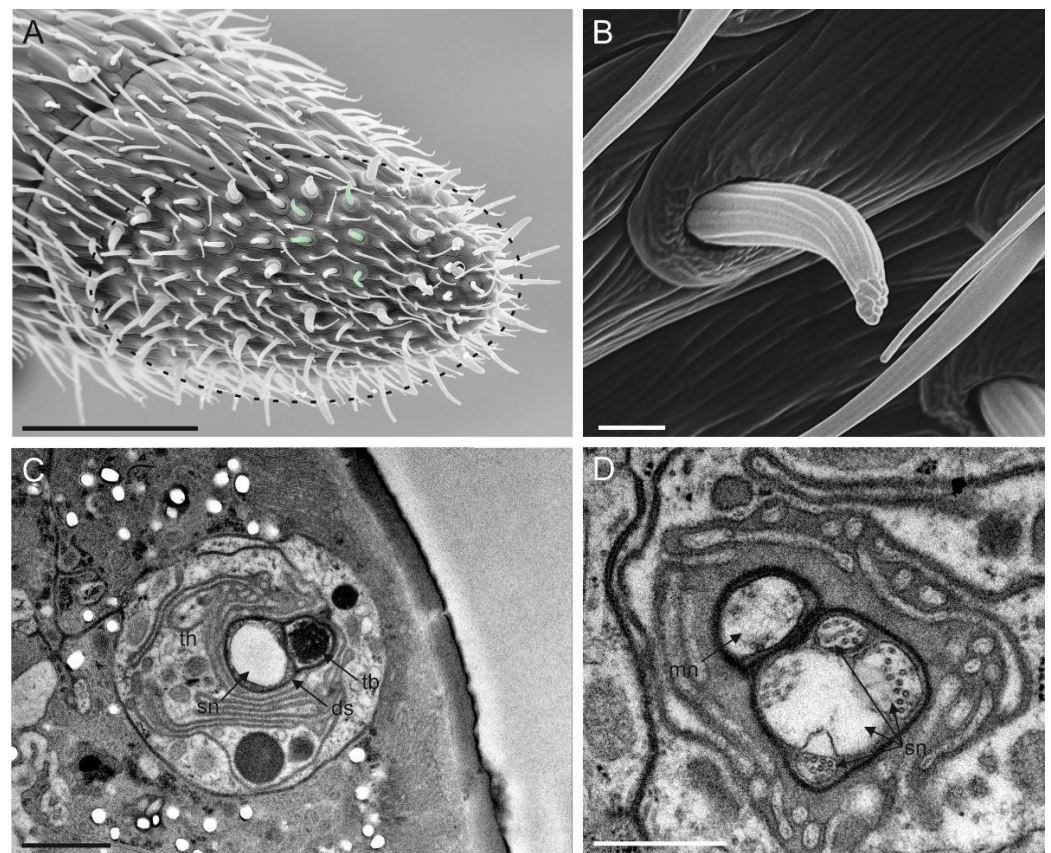


Figure 9. (A) Apical part of the female antennal F7 of *Anagyrus vladimiri* in the ventral view: in the green mask, some of the sensilla chaetica II (SC II) are highlighted. (B) Detail at the SEM of a SC II. (C,D) TEM cross-section showing the sensory neurons (SN) associated with a single SC II. In (C), a more distal section is reported, where a tubular body (tb) and other sensory neurons (sn) are visible, embedded and separated by the dendrite sheath (ds) and the thecogen cell (th). In (D), a more proximal section is shown, reporting the mechanosensory neuron (mn) still separated by the other sn by a distinct ds. Scale bar: (A): 30 μm ; (B,C): 1 μm ; (D): 0.5 μm .

3.9. Sensilla Grooved Peg (SGP)

SGP were the least abundant sensilla present on the flagellum. They were distributed on all antennomeres, positioned on the distal antennomere side (Figure 3). We mapped one SGP on each flagellomere, except the last flagellomere, whereby two SGP were present and positioned dorsally. SGP were inserted on the external cuticle through an evident socket, which appeared to be in the form of a slightly depressed ring (Figure 10A). On average, the sensilla were 3 μm long and 1 μm in diameter. The cuticular base was smooth with no pores, while the apical part of the sensillum was rounded with evident grooves

(Figure 10A,B). Cross-sections taken at the apical part of the sensillum revealed the presence of a thin multiporous wall, with pores located at the grooves base, and therefore, hidden from the outside (Figure 10C). The longitudinal section through the entire shaft revealed the double-walled nature of SGP, with an outermost and innermost cuticular wall (Figure 10B). This latter gave rise to an inner lumen that was occupied by sensory neurons. While at the apical level, we counted up to three outer dendritic segments—sections taken below the SGP socket revealed a total number of five sensory neurons (Figure 10D).

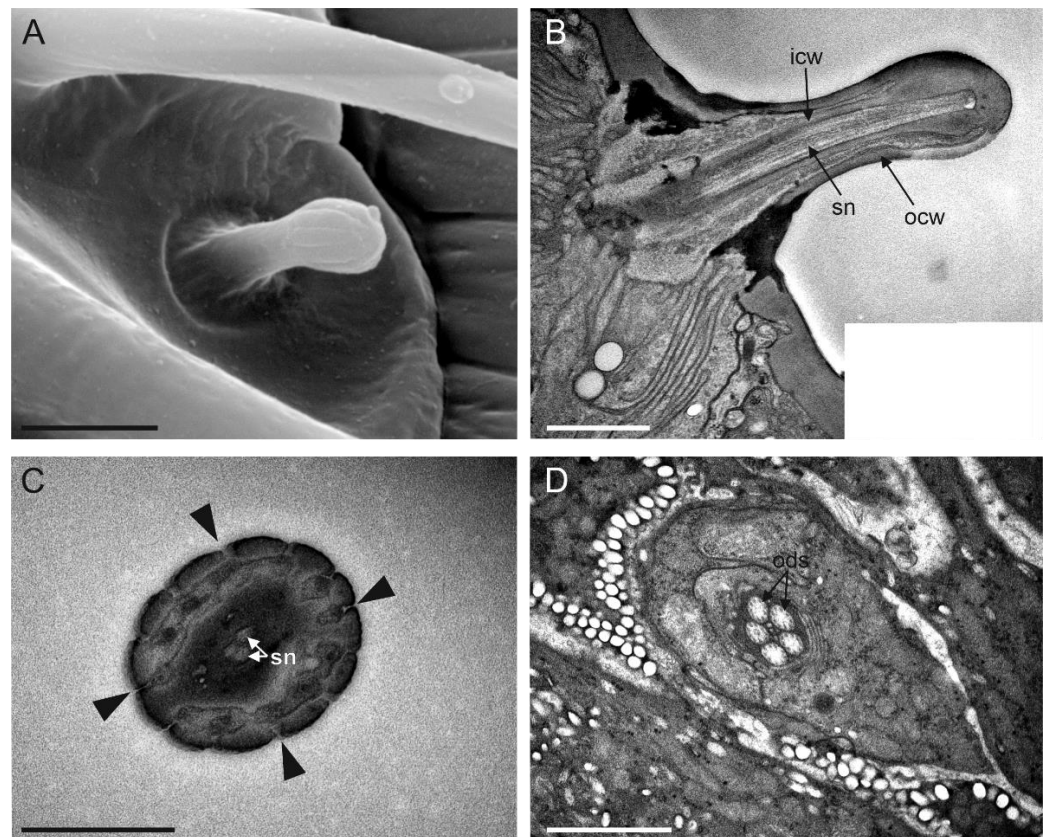


Figure 10. (A) A single sensillum grooved peg (SGP) is visible under SEM, located at the distal margin of F6. The sensillum socket appears slightly sunken, while its distal parts are swollen and longitudinally grooved. (B) TEM picture obtained from 4 different pictures merged together, showing a longitudinal section of an SGP taken from the tip to the base. Two cuticular walls, the outer (ocw) and inner (icw), are visible, with the icw defining an inner lumen occupied by the sensory neurons (sn). (C) TEM cross-section through the sensillum tip showing the grooves and cuticular pores are somehow hidden between them (black arrowheads). Sn are visible in the central part. (D) TEM cross-section taken below the socket level, showing 5 outer dendritic segments (ods) belonging to the sensory neurons associated with a single SGP. Scale bar: (A,D): 2 μ m; (B,C): 1 μ m.

4. Discussion

Encyrtidae is one of the largest families of Chalcidoidea [22]. Their antennae are highly diverse, with flagella appearing from cylindrical to very broad and flat. Although *A. vladimiri* was reported to have a 9-segmented flagellum [14], here we have shown that it is actually composed of 7 segments. This difference is due to the fact that externally, the club appears to be segmented, whereas internally, the last three segments are fused, giving rise to a mono-segmented club. So far, most species belonging to the Encyrtidae were described to present female antennae for which a segmented club was reported [14,23–28]; however, in light of what has been observed in *A. vladimiri*, our hypothesis is that, also in other species belonging to the same family, the occurrence of a mono-segmented club is a common trait.

Similar to what has been reported in several other insect species, the distribution pattern of antennal sensory structures in *A. vladimiri* females follows the tendency to have a greater concentration of sensilla in the apical part of the antennae. Based on their ultrastructural organization, the olfactory, gustatory, mechanosensory and thermohygroreceptive functions have been hypothesized for the different types of antennal sensilla. In the apical part of the antennae, olfactory and gustatory sensilla are mostly found, while mechanosensory structures are more distributed along the antennal length, with no distinct antennomeres that have a specific abundance. The only exception is the apex of the antennae, which uniquely has two types of sensilla, the multiporous basiconic sensilla and the sensilla chaetica II.

Olfactory sensilla are easily distinguished from mechanoreceptor sensilla, mainly because of their perforated cuticular wall, the presence of internally corresponding pore tubules, and the outer dendritic segments of sensory neurons, characterized by a certain level of branching [20,29]. Therefore, based on our morphological investigations, we hypothesize an olfactory role for multiporous plate sensilla (MPS), sensilla trichoidea II (ST II) and sensilla grooved peg (SGP). The MPS and SGP were widely distributed on the flagellomeres, differently from ST II. As for the sensilla number and distribution, this might depend on the level of specialization in terms of the response to different stimuli. In other words, sensilla that are more widely present and distributed over a larger part of the antennal surface could be associated with the perception of “general odours”, or odours of higher importance (e.g., sex pheromone), while those located in a specific area could be tuned to specific groups of volatile or contact chemical compounds [30].

Multiporous plate sensilla (MPS) are a well-documented and rather frequent type of sensilla in Hymenoptera [31–33]. Because of their different external morphology, MPS are often referred to by different names in the literature: porous plates, placoid sensilla, rhinaria, elongate placoid sensilla or multiporous plaque sensilla [32,34,35]. In most families of Hymenoptera Apocrita, MPS are elongated, while in some Vespoidea, Stephanidae and Chrysidoidea, they appear rounded or like small oval plates [33]. In a detailed ultrastructural study of the antennal sensilla of Chalcidoidea, Barlin and Vinson [31] described two types of MPS, which differ in external morphology and cuticular wall thickness. In addition, they studied three species of Encyrtidae, for which they described two types of MPS in females. This contrasts with our results in *A. vladimiri*, where we reported only one type of sensillum, which could be associated with the type I described by Barlin and Vinson. Our observations did not show the presence of a second type of MPS on either the dorsal or ventral side of the antennae. This finding is also confirmed by TEM investigations, which did not reveal the presence of the second type of sensillum, which is characterized by a thick, porous wall. Thus, there seems to be a variation in the presence of MPS types within the different families of Chalcidoidea. No grooves were present around the sensillum, and the tip appeared free of the surrounding antennal cuticle often found in other Chalcidoidea. The internal ultrastructural organization is similar to what has been previously reported. MPS normally have a greater number of associated sensory neurons than those of other sensilla types (frequently more than 20 units). In *Tetrastichus hagenowii* (Ratz) (Eulophidae) and *Torymus warreni* (Cock.) (Torymidae), about 50 sensory neurons have been recorded [31,36], while 25 were recorded in *Dryocosmus kuriphilus* (Cynipidae) [37], 27 in *Itoplectis conquisitor* (Say) (Ichneumonidae) [34], 12–13 in *Coeloide brunneri* Viereck (Braconidae) [38], 37 in *Aphidius smithi* Sharma and Subba Rao (Aphidiidae) [39], and 12–18 in *Apis mellifera* L. (Apidae) [40]. Our finding in *A. vladimiri* of 20 sensory neurons is in line with what has been reported in previous studies. An olfactory function has been proposed for these sensilla, confirmed by electrophysiological studies [41].

Apart from MPS, ST II were also identified as possible olfactory sensilla. This type of sensilla were reported to occur on various insect species [42]. Although the outer cuticular part may show variation among different species (in terms of distribution and abundance of pores), in contrast, its internal organization follows a general pattern typical of an olfactory sensillum. Differently from MPS, ST II were mainly located dorsally on

the apical antennomere and at the distal region of the sub-apical antennomere. The ultrastructural organization was similar to the same sensilla in *Paysandisia archon* (Lepidoptera: Castniidae) [43], *Scleroderma guani* (Bethyridae) [44] and *Eupeodes corollae* (Diptera: Syrphidae) [45]. The occurrence of different types of olfactory sensilla is a common trait that can be found in several insects belonging to diverse, unrelated groups (i.e., Auchenorrhyncha, [46]; Coleoptera, [47,48]; Lepidoptera, [49,50]).

The less abundant sensilla-type is the grooved peg sensilla (GPS), which are normally found as a singular unit on the distal region of the antennomeres. An exception to this pattern was found in the last flagellomere, where we counted two distinct units. This type of sensilla has been reported for several parasitic wasp groups (i.e., Scelionidae [51,52]; Trichogrammatidae [53]; Mymaridae [54]), for which a role in the detection of volatile stimuli was proposed. Similar sensilla occurred also in specialised, blood-sucking species such as mosquitoes [55] and *Triatoma infestans* Klug [56]. In this last species, a different role for double-walled sensilla, regarding the perception of volatiles, has been proposed, with this sensilla more specifically tuned to more polar and hydrophilic volatiles such as short-chain carboxylic acids. Because of this, a possible role in the perception of green leaf volatiles (being mainly composed by hexenal, hexanol and aliphatic organic acids with a chain length of 3–8 carbons) can be hypothesised for *A. vladimiri*.

From a functional point of view, the presence of different types (or subtypes) of olfactory sensilla has been related to the perception of stimuli of various natures linked to the dynamics of intraspecific interaction or related to the host-selection process. In the case of *A. vladimiri*, olfactory sensilla are most likely involved in the perception of host-derived stimuli directly from the host (i.e., sex pheromones) or from plants attacked by the host (induced volatiles).

In *A. vladimiri*, gustatory sensilla were represented by sensilla chaetica type I (SC I) and II (SC II) and multiporous basiconic sensilla (MBS). In general, from a functional point of view, gustatory sensilla frequently combine mechanoreceptive functions with chemoreceptive gustatory functions [20,29], normally associated with the presence of a single apical pore. Some significant exceptions are reported in Hymenoptera parasitoids, with the occurrence of multiporous gustatory sensilla. This type of sensilla is located exclusively on the apical part of the antennae of females, mainly on the ventral side, which allows for contact between the sensilla and the substrate that the insect explores during host-searching behaviour. Ultrastructurally, they consist of truncated-cone-type cuticular elements that apically have spherical projections that touch each other, but are still flexible, so they can move during antennal contact. The apical part is perforated with pores (however, hidden by the spherical projections), while the cuticular wall of the sensilla is poreless. Internally, the multiporous gustatory sensilla harbour a large number of unbranched sensory neurons. These sensilla have been described in Platygastriidae and Scelionidae [57], of which are associated or not with glands. In *Amitus spiniferus* (Platygastriidae), multiporous gustatory sensilla have 220 sensory neurons, while in *Trissolcus basalus*, they reach the impressive number of 400 each [52,57]. In *A. vladimiri*, the MBS are innervated by 20–21 unbranched sensory neurons, a value very different from that reported for Platygastriidae and Scelionidae. A similar reduction in the number of sensory neurons was found in Trichogrammatidae, in which multiporous gustatory sensilla are innervated by 10 neurons [58]. Such differences in the number of neurons could be associated with the number of multiporous sensilla present. In particular, Platygastriidae and Scelionidae have a low number of multiporous gustatory sensilla (whose number does not exceed 10 units per antenna) innervated by a high number of neurons (up to 400 per unit), whereas in *A. vladimiri*, the ventral apical area of females has 25 sensilla, each innervated by 20 neurons. From a functional point of view, in *A. vladimiri*, the role of MBS could be to participate in the various stages of the host-selection process by females, a hypothesis in line with what has been reported for other groups of oophagous parasitoids [59].

Sensilla chaetica type I and II shared a typical ultrastructural organization and topography of gustatory sensilla. In fact, they were located on the distal borders of antennomeres

(SC I), or at the ventral side of the last antennomere (SC II), which enable them to get in contact with the substrate while the insect is antennating. Both sensilla types are equipped with a mechanosensory neuron that can perceive mechanical stimuli. The number of sensory neurons was the same in both sensilla (four gustatory + one mechanoreceptive neuron). A similar number of sensory neurons was found in other insect groups; *Paysandisia archon* (Lepidoptera: Castniidae) [43]; *Eurygaster maura* (Hemiptera: Scutelleridae) [60]; *Dryocosmus kuriphilus* (Hymenoptera: Cynipidae) [36]; *Harmonia axyridis* (Coleoptera: Coccinellidae) [61]; *Psylliodes chrysocephala* (Coleoptera: Chrysomelidae) [62]. In *A. vladimiri*, SCII are exclusively located at the ventral apical tip of the antennae, therefore, sharing the same topographical region occupied by MBS. A similar situation, whereby sensilla that have the same function (contact chemoreception) are located on the same antennal area, was reported for the fruit fly pupal parasitoid *Trichopria drosophilae* Perkins (Hymenoptera: Diapriidae), where the female is equipped with MGS1 and MGS2; the removal of the apical antennomere impaired the ability of the parasitoid to detect its host [63]. These sensilla are known to respond at various compounds found on the substrate. Electrophysiological recordings carried out in different insect species confirmed that these sensilla act as contact chemoreceptors. For example, electrophysiological recordings on *Trissolcus brochymenae* (Hymenoptera: Platygasteridae) showed the response of sensory neurons of sensilla chaetica to various contact stimuli. In addition, a concentration-dependent effect was observed for a few tested compounds, while other compounds had an inhibitory effect on the response of *T. brochymenae* to sugar [64].

On *A. vladimiri* antennae, the major mechanosensory organs were the sensilla trichoidea type I, while sensilla campaniformia and Böhm bristles were located solely at the basal part of the antennae in low numbers. Sensilla trichoidea are a ubiquitous type of sensilla found in different insects. Although the external morphology of sensilla trichoidea is known to differ in length, grooves presence and distribution, their ultrastructural organization is uniform, being made of a sensory neuron ending in a tubular body. For this sensillum, a mechanoreceptive role is hypothesized [29,65–67]. Similarly, campaniform sensilla and Böhm bristles are well known for their proprioceptive mechanosensory function, which can provide information to the insect about the relative position of the antennae during antennation.

Females of *A. vladimiri* were peculiar by having a laterally flattened and enlarged scape—a characteristic commonly reported in Encyrtidae. In other Hymenopterans, the scape is enlarged and sometimes of specific shape, as in the case of the males of *Melittobia australica* Girault [68,69]. These characteristics are usually associated with the specific function that it has on insect biology. For example, the scape of *M. australica* is uniquely shaped in order to clasp the female's antennae tips during courtship. Moreover, the presence of a pheromone-producing gland located within the scape has been reported [68]. Similarly, in several *Aphelinus* species, the presence of antennal pheromone-producing glands has been recorded, and the crucial role of their products in mediating intraspecific communication was hypothesized [70,71]. In our observations, we did not record any cuticular opening on the *A. vladimiri* female scape, which could indicate the presence of glands. Additionally, apart from some sparse sensilla trichoidea I, no other structures were found, which could suggest a functional role of the enlarged scape. Due to its specific colour pattern, the scape may provide cues for species recognition or could absorb heat due to its dark colour.

In Hymenoptera, sexual dimorphism is often observed in social insects and parasitoids. A similar situation was described in *A. vladimiri*, whereby antennal sensilla play a pivotal role in courtship and mating behaviour [72]. The most prominent differences were the general shape of the antennae (lack of the enlarged scape and the presence of long and elongated antennomeres in males), sensilla number and distribution (the presence of long sensilla trichoidea), and the presence of scales on the ventral side on the male apical flagellomeres. The scales on males of *A. vladimiri* were similar to those described in other Encyrtidae: *Leptomastix dactylopii* Howard, *Rhopus meridionalis* (Ferrière) and *Asitus phrag-*

mitis (Ferrière) [73]. Initially, they were described as specialised male sensory structures. However, detailed ultrastructural organization and behavioural investigations confirmed that they actually represent the release sites of epidermal glands, which produce secretions that act as a contact pheromone, necessary to initiate mating, after which they are named as release and spread structures [73].

5. Conclusions

In conclusion, in this study, we reported the ultrastructural organization of the antennal sensilla of female *A. vladimiri*. We showed that the antennae are made of seven antennomeres, with the club being mono-segmented. On the antennae, eight morphologically different sensilla types were recorded, belonging to different functional classes. Among the different types of sensilla, we found two types (MBS and SC II) present only on the female and located in a specific sensory area, for which a role in host recognition was hypothesized. The antennae of males are quite different and have specific structures, for which an involvement in sexual recognition is hypothesized. The present study in fact provides a basis for expanding the study of the functional mechanisms underlying inter- and intraspecific interactions in this important entomophagous species.

Author Contributions: Conceptualization: M.S., P.G., A.L. and R.R.; methodology, M.S., P.G., A.L. and R.R.; validation, M.S., P.G., A.L. and R.R.; formal analysis: M.S., P.G., A.L. and R.R.; investigation: M.S., P.G., A.L. and R.R.; resources: A.L. and R.R.; data curation, M.S., P.G., A.L. and R.R.; writing—original draft preparation: M.S. and R.R.; writing—review and editing: M.S., P.G., A.L. and R.R.; visualization, M.S., P.G., A.L. and R.R.; supervision, A.L. and R.R.; funding acquisition, A.L. and R.R. All authors have read and agreed to the published version of the manuscript.

Funding: This research was funded by the University of Perugia (Fondi di Ateneo).

Institutional Review Board Statement: Ethical review and approval were waived for this study, as investigated species are not considered as laboratory animals according to EU Directive 2010/63.

Informed Consent Statement: Not applicable.

Data Availability Statement: The data that support the findings of this study consist of pictures obtained through SEM and TEM observations. Selected pictures are displayed in the article. All microscopy data are available from the authors upon request.

Acknowledgments: SEM data were obtained at the Scanning Electron Microscopy Centre of DAFE (Pisa University); TEM data were obtained at the Centro Universitario di Microscopia Elettronica e a Fluorescenza (CUMEF; University of Perugia). We also thank Stefano Foschi (Bioplanet srl, Cesena, Italy) for providing live specimens of *A. vladimiri*.

Conflicts of Interest: The authors declare no conflict of interest.

References

1. Miller, D.R.; Miller, G.L.; Watson, G.W. Invasive species of mealybugs (*Hemiptera: Pseudococcidae*) and their threat to U.S. agriculture. *Proc. Entomol. Soc. Wash* **2002**, *104*, 825–836.
2. Lucchi, A.; Suma, P.; Ladurner, E.; Iodice, A.; Savino, F.; Ricciardi, R.; Cosci, F.; Marchesini, E.; Conte, G.; Benelli, G. Managing the vine mealybug, *Planococcus ficus*, through pheromone-mediated mating disruption. *Environ. Sci. Pollut. Res.* **2019**, *26*, 10708–10718. [[CrossRef](#)] [[PubMed](#)]
3. Walton, V.M.; Daane, K.M.; Bentley, W.J.; Millar, J.G.; Larsen, T.E.; Malakar-Kuenen, R. Pheromone-Based mating disruption of *Planococcus ficus* (*Hemiptera: Pseudococcidae*) in California vineyards. *J. Econ. Entomol.* **2006**, *99*, 1280–1290. [[CrossRef](#)] [[PubMed](#)]
4. Bertin, S.; Pacifico, D.; Cavalieri, V.; Marzachì, C.; Bosco, D. Transmission of *Grapevine virus A* and *Grapevine leafroll-associated viruses 1* and *3* by *Planococcus ficus* and *Planococcus citri* fed on mixed-infected plants. *Ann. Appl. Biol.* **2016**, *169*, 53–63. [[CrossRef](#)]
5. Bertin, S.; Cavalieri, V.; Graziano, C.; Bosco, D. Survey of mealybug (*Hemiptera: Pseudococcidae*) vectors of *Ampelovirus* and *Vitivirus* in vineyards of northwestern Italy. *Phytoparasitica* **2010**, *38*, 401–409. [[CrossRef](#)]
6. Mansour, R.; Belzunces, L.P.; Suma, P.; Zappalà, L.; Mazzeo, G.; Grissa-Lebdi, K.; Russo, A.; Biondi, A. Vine and citrus mealybug pest control based on synthetic chemicals. A review. *Agron. Sustain. Dev.* **2018**, *38*, 513. [[CrossRef](#)]
7. Mansour, R.; Grissa Lebdi, K.; Rezgui, S. Assessment of the performance of some new insecticides for the control of the vine mealybug *Planococcus ficus* in a Tunisian vineyard. *Entomol. Hell.* **2010**, *19*, 21–33. [[CrossRef](#)]

8. Cocco, A.; Pacheco da Silva, V.C.; Benelli, G.; Botton, M.; Lucchi, A.; Lentini, A. Sustainable management of the vine mealybug in organic vineyards. *J. Pest. Sci.* **2021**, *94*, 153–185. [[CrossRef](#)]
9. Franco, C.; Suma, P.; Borges da Silva, E.; Blumberg, D.; Mendel, Z. Management strategies of mealybug pests of citrus in Mediterranean Countries. *Phytoparasitica* **2004**, *32*, 507–522. [[CrossRef](#)]
10. Spodek, M.; Ben-Dov, Y.; Mondaca, L.; Protasov, A.; Erel, E.; Mendel, Z. The cotton mealybug, *Phenacoccus solenopsis* Tinsley (Hemiptera: Pseudococcidae) in Israel: Pest status, host plants and natural enemies. *Phytoparasitica* **2018**, *46*, 45–55. [[CrossRef](#)]
11. Kairo, M.T.K.; Pollard, G.V.; Peterkin, D.D.; Lopez, V.F. Biological Control of the Hibiscus Mealybug, *Maconellicoccus hirsutus* Green (Hemiptera: Pseudococcidae) in the Caribbean. *Integr. Pest Manag. Rev.* **2000**, *5*, 241–254. [[CrossRef](#)]
12. Lucchi, A.; Benelli, G. Towards pesticide-free farming? Sharing needs and knowledge promotes Integrated Pest Management. *Environ. Sci. Pollut. Res.* **2018**, *25*, 13439–13445. [[CrossRef](#)] [[PubMed](#)]
13. Noyes, J.S. Universal Chalcidoidea Database. Available online: <https://www.nhm.ac.uk/our-science/data/chalcidoidea/database/index.dsml> (accessed on 8 August 2022).
14. Andreason, S.A.; Triapitsyn, S.V.; Perring, T.M. Untangling the *Anagyris pseudococci* species complex (Hymenoptera: Encyrtidae), parasitoids of worldwide importance for biological control of mealybugs (Hemiptera: Pseudococcidae): Genetic data corroborates separation of two new, previously misidentified species. *Biol. Control.* **2019**, *129*, 65–82. [[CrossRef](#)]
15. Triapitsyn, S.V.; González, D.; Vickerman, D.B.; Noyes, J.S.; White, E.B. Morphological, biological, and molecular comparisons among the different geographical populations of *Anagyris pseudococci* (Hymenoptera: Encyrtidae), parasitoids of *Planococcus* spp. (Hemiptera: Pseudococcidae), with notes on *Anagyris dactylopii*. *Biol. Control.* **2007**, *41*, 14–24. [[CrossRef](#)]
16. Soler, J.M.; Falcó-Garí, J.V.; Herrero, B.; Aquino, D.A. The *Anagyris* (Hymenoptera: Encyrtidae) parasitoids of the obscure mealybug *Pseudococcus viburni* (Hemiptera: Pseudococcidae) in Spain, with description of a new species. *Zootaxa* **2021**, *4980*, 83–98. [[CrossRef](#)] [[PubMed](#)]
17. Ozaki, M.; Wada-Katsumata, A. Perception and Olfaction of Cuticular Compounds. In *Insect Hydrocarbons: Biology, Biochemistry, and Chemical Ecology*; Blomquist, G., Bagnères, A.-G., Eds.; Cambridge University Press: Cambridge, UK, 2010; pp. 207–221.
18. Dicke, M.; van Loon, J.J.A. Multitrophic effects of herbivore-induced plant volatiles in an evolutionary context. *Entomol. Exp. Appl.* **2000**, *97*, 237–249. [[CrossRef](#)]
19. Vet, L.E.M.; Dicke, M. Ecology of infochemical use by natural enemies in a tritrophic context. *Annu. Rev. Entomol.* **1992**, *37*, 141–172. [[CrossRef](#)]
20. Zacharuk, R.Y. Antennae and Sensilla. In *Comprehensive Insect Physiology, Chemistry and Pharmacology*; Kerkut, G.A., Gilbert, L.I., Eds.; Pergamon Press: Oxford, UK, 1985.
21. Fortuna, T.M.; Franco, J.C.; Rebelo, M.T. Morphology and distribution of antennal sensilla in a mealybug parasitoid, *Anagyris* sp. near *pseudococci* (Hymenoptera, Encyrtidae). *Microsc. Microanal.* **2015**, *21*, 8–9. [[CrossRef](#)]
22. Gauld, I.; Bolton, B. *The Hymenoptera*; Oxford University Press: Oxford, UK, 1988; ISBN 0198585217.
23. Guerrieri, E.; Noyes, J.S. Revision of European species of genus *Metaphycus* Mercet (Hymenoptera: Chalcidoidea: Encyrtidae), parasitoids of scale insects (Homoptera: Coccoidea). *Syst. Entomol.* **2000**, *25*, 147–222. [[CrossRef](#)]
24. Rudoy, A.; Zhu, C.D.; Ferrari, R.R.; Zhang, Y.Z. Integrative taxonomy based on morphometric and molecular data supports recognition of the three cryptic species within the *Encyrtus sasakii* complex (Hymenoptera, Encyrtidae). *J. Hymenopt. Res.* **2022**, *90*, 129–152. [[CrossRef](#)]
25. Roh, G.H.; Lee, Y.J.; Zhu, J.J.; Park, C.G. Morphology and distribution of antennal sensilla in egg parasitoid, *Ooencyrtus nezarae* (Hymenoptera: Encyrtidae). *Microsc. Res. Tech.* **2019**, *82*, 972–982. [[CrossRef](#)]
26. Zhou, H.; Wu, W.J.; Zhang, F.P.; Fu, Y.G. Scanning electron microscopy studies of the antennal sensilla of *Metaphycus parasaissetiae* Zhang and Huang (Hymenoptera: Encyrtidae). *Neotrop. Entomol.* **2013**, *42*, 278–287. [[CrossRef](#)] [[PubMed](#)]
27. van Baaren, J.; Barbier, R.; Nénon, J.P. Female antennal sensilla of *Epidinocarsis lopezi* and *Leptomastix dactylopii* (Hymenoptera: Encyrtidae), parasitoids of pseudococcid mealybugs. *Can. J. Zool.* **1996**, *74*, 710–720. [[CrossRef](#)]
28. Xi, Y.-Q.; Yin, X.-M.; Zhu, C.-D.; Guerrieri, E.; Zhang, Y.-Z. Scanning electron microscopy studies of antennal sensilla of *Ooencyrtus phongi* (Hymenoptera: Encyrtidae). *Microsc. Res. Tech.* **2011**, *74*, 936–945. [[CrossRef](#)] [[PubMed](#)]
29. Keil, T.A.; Steinbrecht, R.A. Mechanosensitive and Olfactory Sensilla of Insects. In *Insect Ultrastructure*; King, R.C., Akai, H., Eds.; Springer: Boston, MA, USA, 1984; pp. 477–516.
30. Schmidt, H.R.; Benton, R. Molecular mechanisms of olfactory detection in insects: Beyond receptors. *Open Biol.* **2020**, *10*, 200252. [[CrossRef](#)] [[PubMed](#)]
31. Barlin, M.R.; Bradleigh Vinson, S. Multiporous plate sensilla in antennae of the Chalcidoidea (Hymenoptera). *Int. J. Insect Morphol. Embryol.* **1981**, *10*, 29–42. [[CrossRef](#)]
32. Basibuyuk, H.H.; Quicke, D.L.J. Gross morphology of multiporous plate sensilla in the Hymenoptera (Insecta). *Zool. Scr.* **1999**, *28*, 51–67. [[CrossRef](#)]
33. Polidori, C.; Nieves-Aldrey, J.L. Diverse filters to sense: Great variability of antennal morphology and sensillar equipment in gall-wasps (Hymenoptera: Cynipidae). *PLoS ONE* **2014**, *9*, e101843. [[CrossRef](#)]
34. Borden, J.H.; Chong, L.; Rose, A. Morphology of the elongate placoid sensillum on the antennae of *Itopectis conquisitor*. *Ann. Entomol. Soc. Am.* **1978**, *71*, 223–227. [[CrossRef](#)]
35. Onagbola, E.O.; Boina, D.R.; Hermann, S.L.; Stelinski, L.L. Antennal Sensilla of *Tamarixia radiata* (Hymenoptera: Eulophidae), a Parasitoid of *Diaphorina citri* (Hemiptera: Psyllidae). *Ann. Entomol. Soc. Am.* **2009**, *102*, 523–531. [[CrossRef](#)]

36. Barlin, M.R.; Bradleigh Vinson, S.; Piper, G.L. Ultrastructure of the antennal sensilla of the cockroach-egg parasitoid, *Tetrastichus hagenowii* (Hymenoptera: Eulophidae). *J. Morphol.* **1981**, *168*, 97–108. [[CrossRef](#)] [[PubMed](#)]
37. Sevarika, M.; Stacconi, M.V.R.; Romani, R. Fine morphology of antennal and ovipositor sensory structures of the gall chestnut wasp, *Dryocosmus kuriphilus*. *Insects* **2021**, *12*, 231. [[CrossRef](#)] [[PubMed](#)]
38. Richerson, J.V.; Borden, J.H.; Hollingdale, J. Morphology of a unique sensillum placodeum on the antennae of *Coeloides brunneri* (Hymenoptera: Braconidae). *Can. J. Zool.* **1972**, *50*, 909–913. [[CrossRef](#)]
39. Borden, J.H.; Rose, A.; Chorney, R.J. Morphology of the elongate sensillum placodeum on the antennae of *Aphidius smithi* (Hymenoptera: Aphidiidae). *Can. J. Zool.* **1978**, *56*, 519–525. [[CrossRef](#)]
40. Slifer, E.H.; Sekhon, S.S. Fine structure of the sense organs on the antennal flagellum of the honey bee, *Apis mellifera* Linnaeus. *J. Morphol.* **1961**, *109*, 351–381. [[CrossRef](#)]
41. Kaissling, K.-E.; Renner, M. Antennale Rezeptoren für Queen Substance und Sterzelduft bei der Honigbiene. *Z. Vgl. Physiol.* **1968**, *59*, 357–361. [[CrossRef](#)]
42. Chang, H.; Guo, M.; Wang, B.; Liu, Y.; Dong, S.; Wang, G. Sensillar expression and responses of olfactory receptors reveal different peripheral coding in two *Helicoverpa* species using the same pheromone components. *Sci. Rep.* **2016**, *6*, 8742. [[CrossRef](#)]
43. Ruschioni, S.; Riolo, P.; Verdolini, E.; Peri, E.; Guarino, S.; Colazza, S.; Romani, R.; Isidoro, N. Fine structure of antennal sensilla of *Paysandisia archon* and electrophysiological responses to volatile compounds associated with host palms. *PLoS ONE* **2015**, *10*, e0124607. [[CrossRef](#)]
44. Li, X.; Lu, D.; Liu, X.; Zhang, Q.; Zhou, X. Ultrastructural Characterization of Olfactory Sensilla and Immunolocalization of Odorant Binding and Chemosensory Proteins from an Ectoparasitoid *Scleroderma guani* (Hymenoptera: Bethylinidae). *Int. J. Biol. Sci.* **2011**, *7*, 848–868. [[CrossRef](#)]
45. Dong, W.Y.; Wang, B.; Wang, G.R. Morphological and ultrastructural characterization of antennal sensilla and the detection of floral scent volatiles in *Eupeodes corollae* (Diptera: Syrphidae). *Front. Neuroanat.* **2021**, *15*, 1900. [[CrossRef](#)]
46. Riolo, P.; Minuz, R.L.; Anfora, G.; Stacconi, M.V.R.; Carlin, S.; Isidoro, N.; Romani, R. Perception of host plant volatiles in *Hyalesthes obsoletus*: Behavior, morphology, and electrophysiology. *J. Chem. Ecol.* **2012**, *38*, 1017–1030. [[CrossRef](#)] [[PubMed](#)]
47. Merivee, E.; Rahi, M.; Bresciani, J.; Ravn, H.P.; Luik, A. Antennal sensilla of the click beetle, *Limonius aeruginosus* (Olivier) (Coleoptera: Elateridae). *Int. J. Insect Morphol. Embryol.* **1998**, *27*, 311–318. [[CrossRef](#)]
48. di Giulio, A.; Maurizi, E.; Rossi Stacconi, M.V.; Romani, R. Functional structure of antennal sensilla in the myrmecophilous beetle *Paussus favieri* (Coleoptera, Carabidae, Paussini). *Micron* **2012**, *43*, 705–719. [[CrossRef](#)] [[PubMed](#)]
49. Li, Y.; Liu, F.; Du, X.; Li, Z.; Wu, J. Ultrastructure of antennal sensilla of three fruit borers (Lepidoptera: Crambidae or Tortricidae). *PLoS ONE* **2018**, *13*, e0205604. [[CrossRef](#)] [[PubMed](#)]
50. Larsson, M.C.; Hallberg, E.; Kozlov, M.V.; Francke, W.; Hansson, B.S.; Löfstedt, C. Specialized olfactory receptor neurons mediating intra- and interspecific chemical communication in leafminer moths *Eriocrania* spp. (Lepidoptera: Eriocraniidae). *J. Exp. Biol.* **2002**, *205*, 989–998. [[CrossRef](#)]
51. Cave, R.D.; Gaylor, M.J. Antennal sensilla of male and female *Telenomus reynoldsi* Gordh and Coker (Hymenoptera: Scelionidae). *Int. J. Insect Morphol. Embryol.* **1987**, *16*, 27–39. [[CrossRef](#)]
52. Bin, F.; Colazza, S.; Isidoro, N.; Solinas, M.; Vinson, S.B. Antennal chemosensilla and glands, and their possible meaning in the reproductive behaviour of *Trissolcus basalis* (Woll.) (Hym.: Scelionidae). *Entomologica* **1989**, *24*, 33–97.
53. Amornsak, W.; Cribb, B.; Gordh, G. External morphology of antennal sensilla of *Trichogramma australicum* Girault (Hymenoptera: Trichogrammatidae). *Int. J. Insect Morphol. Embryol.* **1998**, *27*, 67–82. [[CrossRef](#)]
54. van Baaren, J.; Boivin, G.; le Lannic, J.; Nénon, J.-P. Comparison of antennal sensilla of *Anaphes victus* and *A. listronoti* (Hymenoptera, Mymaridae), egg parasitoids of Curculionidae. *Zoomorphology* **1999**, *119*, 76. [[CrossRef](#)]
55. McIver, S.B. Fine structure of antennal grooved pegs of the mosquito, *Aedes aegypti*. *Cell Tissue Res.* **1974**, *153*, 9162. [[CrossRef](#)]
56. Diehl, P.A.; Vlimant, M.; Guerenstein, P.; Guerin, P.M. Ultrastructure and receptor cell responses of the antennal grooved peg sensilla of *Triatoma infestans* (Hemiptera: Reduviidae). *Arthropod. Struct. Dev.* **2003**, *31*, 271–285. [[CrossRef](#)] [[PubMed](#)]
57. Isidoro, N.; Romani, R.; Bin, F. Antennal multiporous sensilla: Their gustatory features for host recognition in female parasitic wasps (Insecta, Hymenoptera: Platygastroidea). *Microsc. Res. Tech.* **2001**, *55*, 350–358. [[CrossRef](#)] [[PubMed](#)]
58. Ruschioni, S.; Romani, R.; Romani, R.O. Morphology and distribution of antennal multiporous gustatory sensilla related to host recognition in some *Trichogramma* spp. *Bull. Insectolog.* **2012**, *65*, 171–176.
59. Isidoro, N.; Bin, F.; Colazza, S.; Vinson, S.B. Morphology of antennal gustatory sensilla and glands in some parasitoid Hymenoptera with hypothesis on their role in sex and host recognition. *J. Hymenopt. Res.* **1996**, *5*, 206–239.
60. Romani, R.; Rossi Stacconi, M.V. Mapping and ultrastructure of antennal chemosensilla of the wheat bug *Eurygaster maura*. *Insect Sci.* **2009**, *16*, 193–203. [[CrossRef](#)]
61. Sevarika, M.; Rondoni, G.; Conti, E.; Romani, R. Antennal sensory organs and glands of the harlequin ladybird, *Harmonia axyridis*. *Entomol. Exp. Appl.* **2021**, *169*, 111–124. [[CrossRef](#)]
62. Isidoro, N.; Bartlett, E.; Ziesmann, J.; Williams, I.H. Antennal contact chemosensilla in *Psylliodes chrysocephala* responding to cruciferous allelochemicals. *Physiol. Entomol.* **1998**, *23*, 131–138. [[CrossRef](#)]
63. Romani, R.; Isidoro, N.; Bin, F.; Vinson, S.B. Host recognition in the pupal parasitoid *Trichopria drosophilae*: A morpho-functional approach. *Entomol. Exp. Appl.* **2002**, *105*, 119–128. [[CrossRef](#)]

64. Iacovone, A.; Salerno, G.; French, A.S.; Conti, E.; Marion-Poll, F. Antennal gustatory perception and behavioural responses in *Trissolcus brochymenae* females. *J. Insect Physiol.* **2015**, *78*, 15–25. [[CrossRef](#)]
65. McIver, S.B. Mechanoreception. *Compr. Insect Physiol. Biochem. Pharmacol.* **1985**, *6*, 71–132.
66. Keil, T.A. Functional morphology of insect mechanoreceptors. *Microsc. Res. Tech.* **1997**, *39*, 506–531. [[CrossRef](#)]
67. Krishnan, A.; Sane, S.P. Antennal Mechanosensors and Their Evolutionary Antecedents. In *Advances in Insect Physiology*; Elsevier Ltd.: Amsterdam, The Netherlands, 2015; Volume 49, pp. 59–99.
68. Dahms, E.C. An interpretation of the structure and function of the antennal sense organs of *Melittobia australica* (Hymenoptera: Eulophidae) with the discovery of a large dermal gland in the male scape. *Mem. Queensl. Mus.* **1984**, *21*, 361–385.
69. Matthews, R.W.; González, J.M.; Matthews, J.R.; Deyrup, L.D. Biology of the Parasitoid *Melittobia* (Hymenoptera: Eulophidae)*. *Annu. Rev. Entomol.* **2009**, *54*, 251–266. [[CrossRef](#)] [[PubMed](#)]
70. Romani, R.; Grasso, D.A.; Mori, A.; Isidoro, N.; Moli, F. le Antennal glands of the slave-making ant *Polyergus. rufescens* and its slave species *Formica cunicularia* (Hymenoptera, Formicidae). *Can. J. Zool.* **2006**, *84*, 490–494. [[CrossRef](#)]
71. Shirley, X.A.; Woolle, J.B.; Hoppe, K.R.; Isidoro, N.; Romani, R. Evolution of glandular structures on the scape of males in the genus *Aphelinus* Dalman (Hymenoptera, Aphelinidae). *J. Hymenopt. Res.* **2019**, *72*, 27–43. [[CrossRef](#)]
72. Romano, D.; Benelli, G.; Stefanini, C.; Desneux, N.; Ramirez-Romero, R.; Canale, A.; Lucchi, A. Behavioral asymmetries in the mealybug parasitoid *Anagyris* sp. near *pseudococci*: Does lateralized antennal tapping predict male mating success? *J. Pest Sci.* **2018**, *91*, 341–349. [[CrossRef](#)]
73. Guerrieri, E.; Pedata, P.A.; Romani, R.; Isidoro, N.; Bin, F. Functional anatomy of male antennal glands in three species of Encyrtidae (Hymenoptera: Chalcidoidea). *J. Nat. Hist.* **2001**, *35*, 41–54. [[CrossRef](#)]